https://doi.org/10.31436/iiumej.v27i2.4013

Analytical and Flight Test-Based Dynamic Characteristic Identification of a Small Fixed-Wing UAV

ERIES BAGITA JAYANTI[1*], YAZDI IBRAHIM JENIE[2], ARDIAN RIZALDI[1,3], NOVITA ATMASARI[1], FUAD SURASTYO PRANOTO[1]

[1]*Research Center for Aeronautics Technology, National Research and Innovation Agency, Bogor, Indonesia*
[2]*Aerospace Engineering, Faculty of Mechanical and Aerospace Engineering, Institut Teknologi Bandung, Bandung, Indonesia*
[3]*Aerospace Engineering, Graduate School of Mechanical and Aerospace Engineering, Gyeongsang National University, Jinju, Gyeongsangnam-do, Korea*

**Corresponding author: erie002@brin.go.id*

(Received: 27 October 2025; Accepted: 9 March 2026; Published online: 10 May 2026)

ABSTRACT: Reliable and efficient UAV flight control design requires accurate knowledge of the vehicle's dynamic characteristics, which are rarely provided by manufacturers and must therefore be determined independently. These characteristics can be obtained through analytical calculations, wind tunnel testing, and flight testing. However, in small UAV development, the process is often simplified by skipping directly to flight tests for control tuning, without first examining the underlying dynamic behavior. To address this gap, this research compares the dynamic characteristics derived from analytical calculations and flight testing. The case study focuses on BRIN's bMFE-UAV, in which longitudinal and lateral/directional dynamics are identified using control-surface deflections as inputs and measured responses of speed, altitude, attitude, acceleration, and rotational rate as outputs. Results reveal consistent oscillatory behaviors: two oscillatory modes in longitudinal dynamics and, in lateral/directional dynamics, one oscillatory mode accompanied by two non-oscillatory modes. Only the damping ratio of the short-period mode showed close agreement (<10% difference), while other parameters exhibited substantial discrepancies. The discrepancies demonstrate the limitations of analytical methods in accurately reflecting real flight dynamics, reinforcing the necessity of flight testing to ensure reliable data for small UAV flight-control design.

ABSTRAK: Reka bentuk kawalan penerbangan UAV yang boleh dipercayai dan cekap memerlukan pengetahuan tepat pada ciri dinamik kenderaan. Ianya jarang didapati daripada pengeluar dan oleh itu mesti ditentukan secara bebas. Ciri-ciri ini boleh diperolehi melalui pengiraan analitika, ujian terowong angin, dan ujian penerbangan. Walau bagaimanapun, dalam pembangunan UAV kecil, prosesnya sering dipermudahkan dengan melangkau terus ke ujian penerbangan bagi kawalan penalaan, tanpa terlebih dahulu memeriksa tingkah laku dinamik. Kajian ini bertujuan membandingkan ciri dinamik yang diperoleh daripada pengiraan analitika dan ujian penerbangan. Kajian kes memfokuskan pada bMFE-UAV BRIN, di mana dinamik membujur dan sisi/arah dikenal pasti menggunakan pesongan permukaan kawalan sebagai input dan tindak balas diukur pada kelajuan, ketinggian, sikap, pecutan dan kadar putaran sebagai hasil pengeluaran. Dapatan mendapati tingkah laku berayun yang konsisten: dua mod berayun dalam dinamik membujur dan dalam dinamik sisi/arah, satu mod berayun disertai dengan dua mod bukan berayun. Hanya nisbah redaman mod jangka pendek menunjukkan perbezaan terdekat (iaitu <10%), manakala parameter lain menunjukkan ralat yang besar. Ralat menunjukkan batasan kaedah analisis dalam

mencerminkan dinamik penerbangan sebenar, mengukuhkan keperluan ujian penerbangan bagi memastikan data boleh dipercayai untuk reka bentuk kawalan penerbangan UAV kecil.

KEYWORDS: *Dynamic Characteristic Identification, Dynamic Modeling, Flight Test, UAV*

1. INTRODUCTION

Accurate knowledge of UAV dynamic characteristics is essential for the design of reliable and efficient flight control systems. However, UAV manufacturers rarely provide such data, necessitating independent investigations. The three most common methods for gathering aircraft dynamic characteristics are analytical calculations, wind-tunnel testing, and flight testing. The analytical calculation, using available software such as the USAF DATCOM or Computational Fluid Dynamics (CFD), involves many assumptions and simplifications, leading to inaccurate results [1, 2]. However, this method is the quickest, safest, and cheapest of the three and is ideal for preliminary research [3, 4]. Utilizing a wind tunnel and a scaled model enables more accurate aerodynamic data to be obtained. It can be used to derive dynamic characteristics data [5, 6]. However, Wind Tunnel testing is expensive and time-consuming, not to mention the rarity of the facilities. The third method is to conduct flight tests directly, gathering the aircraft's dynamic characteristics in the actual flight environment. While this method is considered the most accurate, it requires considerably more resources and time, and poses greater risks to the aircraft, pilots, and the environment [7, 8].

In crewed aircraft development, these methods are commonly used in succession, from the quickest and cheapest to the most time-consuming and expensive. The resulting data is updated continuously once results from more accurate methods are obtained. However, the paradigm changes in small UAV development. The development costs and operational risks are much lower. Typically, small UAV developers skip complex analysis and wind-tunnel testing, proceeding directly to flight testing and iterating on the vehicle control design based on experience [9]. Many failures that destroy prototypes are common during the iteration, yet still cheaper than conducting a rigorous derivation, as in crewed aircraft development. Nevertheless, the process skips many engineering steps, including deriving dynamic characteristics. The lack of documentation, resulting from skipped steps, also invalidates the control system design and hinders further development [10]. This condition somewhat contradicts the role of flight testing, which is generally regarded as the most accurate method for deriving dynamic characteristics. These characteristics are typically used as the basis for flight control system design. Therefore, a direct comparison between analytically derived dynamic characteristics and those obtained from flight-test-based identification is necessary to assess the reliability and applicability of analytical models for small UAVs.

Based on this motivation, the objective of this research is to perform a comparative analysis of UAV dynamic characteristics obtained from analytical calculations and flight test-based identification. Such a methodology has been demonstrated frequently in many studies [11-13], but is rarely applied in small-UAV development, which often relies on trial and error to determine appropriate control gains. The case study in this research is the MFE surveillance UAV owned by the National Research and Innovation Agency (BRIN), hereafter referred to as the bMFE-UAV. Its dynamic characteristics are identified along both the longitudinal and lateral/directional axes using recorded flight-test data [13-15]. The deflections of the UAV control surfaces, including its elevator and ailerons, are used as input variables, while the recorded IMU and other sensor data, including vehicle speed, altitude, attitude, acceleration, and rotational rate, serve as the output for the identification process. The results are then compared with analytical data obtained using the USAF DATCOM software.

https://doi.org/10.31436/iiumej.v27i2.4013

This article is structured as follows. The case study UAV will be explained along with its specifications. Afterward, the vehicle dynamic characteristics are derived by first determining its mathematical model, and aerodynamic data is obtained using the USAF DATCOM. Then, it describes the vehicle's flight test process, the essential data obtained, and the identification process that used Ordinary Least Squares analysis. All the results are then compared, and the research concludes with several suggestions.

2. METHODOLOGY

2.1. Case Study: bMFE-UAV

Figure 1 shows the bMFE-UAV used in this study, a twin-engine fixed-wing aircraft with a conventional configuration.

Figure 1. bMFE-UAV.

The UAV is powered by two electric engines that drive two propellers on its wings. The motion of rolling, pitching, and yawing is actuated by its ailerons on its wing and elevators and rudder on its T-Tail configured stabilizer. The UAV is mainly made of Styrofoam, with polymer reinforcement at the joints and in its engine compartment. It is widely used in topographical mapping, land surveying, precision farming, environmental monitoring, and many other missions. Table 1 lists further specifications of the bMFE-UAV [16].

Table 1. Specification of UAV

Specifications	Symbol	Value
Wingspan	b	2.43 m
Wing Area	S	0.75 m^2
Mean Aerodynamic Chord	$\bar{c}$	0.3 m
Horizontal tail area	S_H	0.07 m^2
Vertical tail area	S_V	0.065 m^2
Max. Take-off Weight	MTOW	11.5 kg
Suggested payload	$m_{payload}$	< 2.5 kg
Cruise flight speed	V	17-20 m/s
Cruising altitude	h	300 m
Longest flight range	RNG	150 km
Moment of inertia around x axis	I_x	0.8244 kg.m^2
Moment of inertia around y axis	I_y	1.1350 kg.m^2
Moment of inertia around z axis	I_z	0.1723 kg.m^2
Moment of inertia in xz axis	I_{xz}	0.1266 kg.m^2

https://doi.org/10.31436/iiumej.v27i2.4013

2.2. Dynamics Characteristics Derivation by Analytical Calculations

This section explains the dynamic characteristics derived from analytical methods, primarily based on data computed with the USAF DATCOM software.

2.2.1. Aircraft Equation of Motion

The equation of motion of any moving body (including Aircraft) is derived from Newton's Laws of Motion for a six degrees of freedom (6-DOF) motion in the Three-Dimensional Space [17]. These are sets of translational and rotational equations of motion, accompanied by kinematic equations, represented in Eqs. (1), (2), and (3), respectively. All vectors are defined in the aircraft stability axis on cruising conditions.

$$\frac{d\bar{V}}{dt} = \frac{\sum \bar{F}}{m} - \bar{\omega} \times \bar{V} \tag{1}$$

$$\frac{d\bar{\omega}}{dt} = \boldsymbol{I}^{-1}[\sum \bar{M} - \bar{\omega} \times \boldsymbol{I}\bar{\omega}] \tag{2}$$

$$\begin{bmatrix} \dot{\varphi} \\ \dot{\theta} \\ \dot{\psi} \end{bmatrix} = \begin{bmatrix} 1 & sin\,\varphi\, tan\,\theta & cos\,\varphi\, tan\,\theta \\ 0 & cos\,\varphi & -sin\,\varphi \\ 0 & \frac{sin\,\varphi}{cos\,\theta} & \frac{cos\,\varphi}{cos\,\theta} \end{bmatrix} \bar{\omega} \tag{3}$$

where the vectors of translational and rotational rates are defined as:

$$\bar{V} = [u \quad v \quad w]^T \tag{4}$$

and,

$$\bar{\omega} = [p \quad q \quad r]^T \tag{5}$$

Mass (m) is assumed to be constant during the analysis and set to the actual flight-test weight in Table 5. The moment of inertia (I) is a tensor matrix defined as in Eq. (6), where the polar inertia is listed in Table 1, and all cross-inertias are assumed to be zero, except for I_{xz}.

$$\boldsymbol{I} = \begin{bmatrix} I_x & -I_{xy} & -I_{xz} \\ -I_{xy} & I_y & -I_{yz} \\ -I_{xz} & -I_{yz} & I_z \end{bmatrix} \tag{6}$$

The forces and moments acting on the aircraft are modeled as a summation of the aspects of aerodynamics, propulsion, and gravitational (weight), as in Eq. (7) and Eq. (8), referred to by the superscripts A, P, and W, respectively.

$$\sum \bar{F} = \bar{F}^A + \bar{F}^P + \bar{F}^W \tag{7}$$

$$\sum \bar{M} = \bar{M}^A + \bar{M}^P \tag{8}$$

The sum of moments in Eq. (8) is formulated based on the aircraft's center of gravity. As a result, weight does not contribute to the moment and is therefore excluded from the moment equation.

These forces and moments are detailed in the following paragraphs:

a. Aerodynamics

The bMFE-UAV aerodynamic forces and moments are modeled in Eq. (9) and Eq. (10). S denotes the reference or wing planform area, $\bar{c}$ and b is the mean aerodynamic chord and wingspan length, and V denotes the vehicle airspeed. The values of those parameters are listed in Table 1.

https://doi.org/10.31436/iiumej.v27i2.4013

Eq. (9) is initially formulated in the aerodynamic axis system and subsequently transformed into the body axis using the transformation matrix defined in Eq. (11). In this formulation, the aerodynamic lift and drag directions are defined opposite to the positive body-axis directions, whereas the side force follows the positive body y-axis convention.

$$\bar{F}^A = \frac{1}{2}\rho V^2 S\, C_b^a \begin{bmatrix} C_D\{\alpha\} \\ C_Y\{\beta, \delta_a\} \\ C_L\{\alpha, \delta_e\} + C_{L_q}\frac{\bar{c}}{2V}q \end{bmatrix} \tag{9}$$

$$\bar{M}^A = \frac{1}{2}\rho V^2 S \begin{bmatrix} b\left(C_\ell\{\beta, \delta_a\} + C_{\ell_p}\frac{b}{2V}p + C_{\ell_r}\frac{b}{2V}r\right) \\ \bar{c}\left(C_m\{\alpha, \delta_e\} + C_{m_q}\frac{\bar{c}}{2V}q\right) \\ b\left(C_n\{\beta, \delta_a\} + C_{n_p}\frac{b}{2V}p + C_{n_r}\frac{b}{2V}r\right) \end{bmatrix} \tag{10}$$

$$C_b^a = \begin{bmatrix} -\cos\alpha\cos\beta & -\cos\alpha\sin\beta & \sin\alpha \\ -\sin\beta & -\cos\beta & 0 \\ -\sin\alpha\cos\beta & -\sin\alpha\sin\beta & -\cos\alpha \end{bmatrix} \tag{11}$$

In this study, the aerodynamic model formulation conceptually accounts for rudder effects; however, rudder-related aerodynamic derivatives are not estimated. This is because the flight test campaign did not include deliberate rudder excitation, resulting in insufficient excitation for reliable parameter identification. Consequently, rudder contributions are not explicitly included in Eq. (9) and Eq. (10).

The symbol ρ denotes the atmospheric density, which this research will use the value 1.18 kg/m3, representing the UAV cruising altitude at 300 m. The forces in Eq. (9) undergo axis transformation into the aircraft body axis, via the transformation matrix, C_b^a, presented in Eq. (11). The aerodynamic derivatives in Eq. (9) and Eq. (10) include the effect of steady-state and perturbed flight conditions. The steady-state coefficients are the derivatives for forces of drag, side force, and lift, or C_D, C_Y, and C_L, and the derivatives for moments of rolling, pitching, and yawing, or C_ℓ, C_m, and C_n, respectively. The value for these coefficients depends on the steady-state flight conditions: the angle of attack (α) and the side slip angle (β), and the steady-state control input: the elevator deflection (δ_e) and aileron deflection (δ_a).

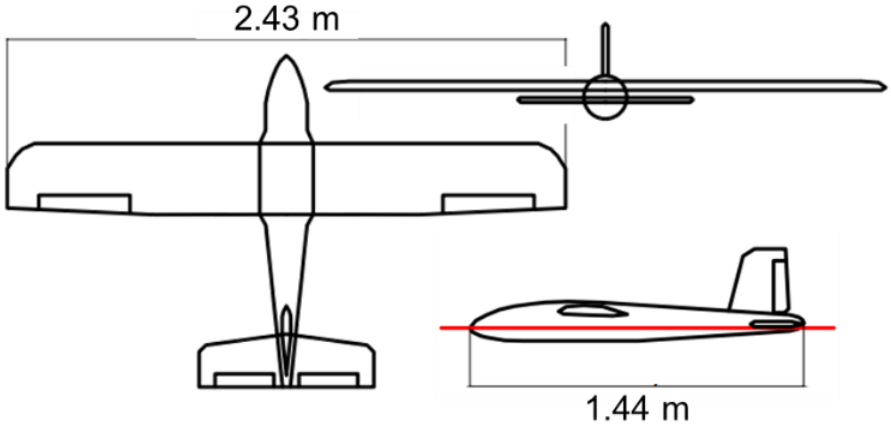

Figure 2. Three-view drawing of UAV, simplified for DATCOM.

Eq. (9) and Eq. (10) also account for aerodynamics under perturbed flight conditions, represented by the dynamic derivatives of force and moment with respect to the rotational rates

https://doi.org/10.31436/iiumej.v27i2.4013

(p, q, and r). These include the lift and pitching-moment derivatives with respect to the pitch rate, and the rolling and yawing moment derivatives with respect to the roll and yaw rates. Those aerodynamic derivatives are obtained using the USAF Digital DATCOM software, which requires the geometric description of bMFE-UAV configurations and flight conditions. The outputs will be the complete set of dimensionless aerodynamic derivatives required for Eqs. (9) and (10). The basic geometry of the bMFE-UAV is listed in Table 1, which shows the conventional configuration comprising a fuselage, wing, horizontal tailplane, and vertical tailplane. Other dimensions and configurations required for DATCOM input were obtained by direct measurement of the vehicle and from the three-view drawing in **Figure 2**.

Figure 3 (a) to (c) depict the results of longitudinal aerodynamic derivatives due to variation of the angle of attack (α), in various elevator deflection (δ_e). **Figure 4** (a) to (c), on the other hand, shows the lateral/directional due to the side slip angles (β). Only the roll coefficient (C_ℓ) is affected by the aileron deflection (δ_a).

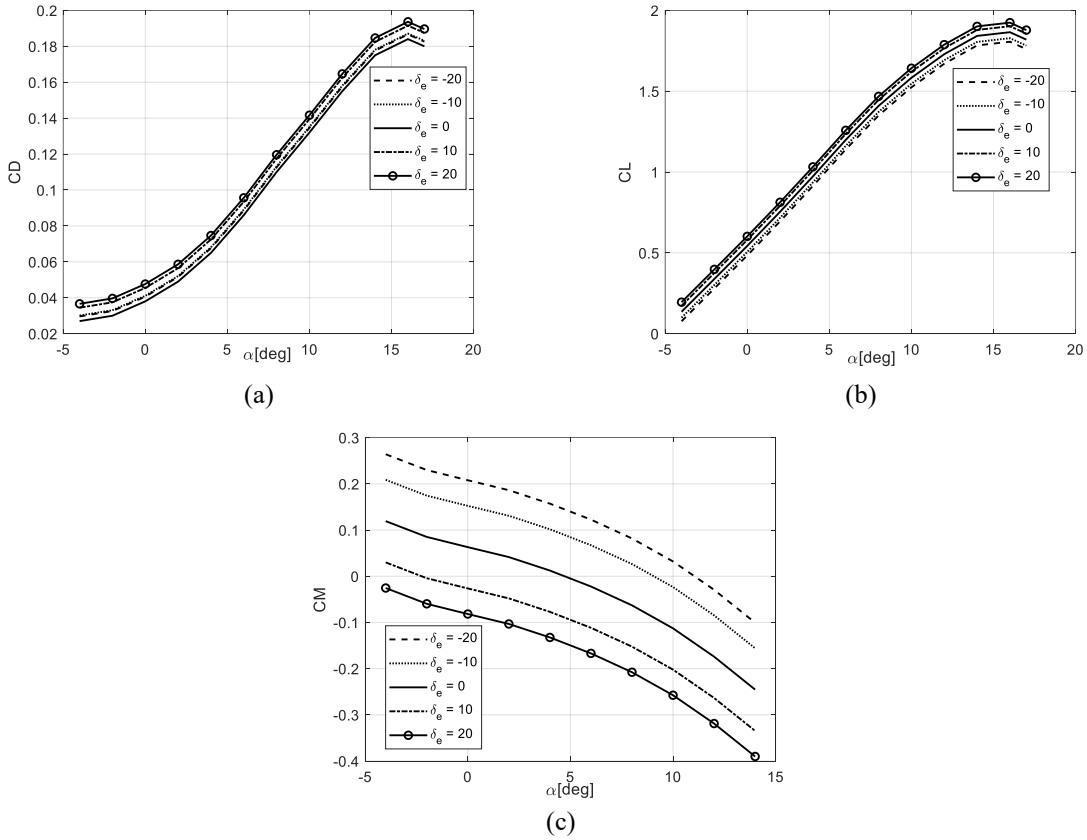

(a) (b)

(c)

Figure 3. Aerodynamic characteristics of the bMFE-UAV, including the (a) Lift force coefficient; (b) Drag force coefficient; (c) Pitch moment coefficient.

The dynamic derivatives in longitudinal and lateral/directional modes are presented in Table 2, with the symbols used in Eqs. (9) and (10). These values are assumed to be constant within the flight-condition dynamics during the analysis. Other rotational-rate effects on the forces and moments may also occur, but are assumed to be insignificant and neglected.

https://doi.org/10.31436/iiumej.v27i2.4013

Table 2. Dynamics Derivatives Coefficient

Parameter	Symbol	Value [./rad]
Lift derivative due to the pitching rate	C_{L_q}	6.145
Pitch moment derivative due to the pitching rate	C_{m_q}	-11.236
Roll moment derivative due to the rolling rate	C_{ℓ_p}	-0.513
Roll moment derivative due to the yawing rate	C_{ℓ_r}	0.149
Yaw moment derivative due to the rolling rate	C_{n_p}	-0.044
Yaw moment derivative due to the yawing rate	C_{n_r}	-0.046

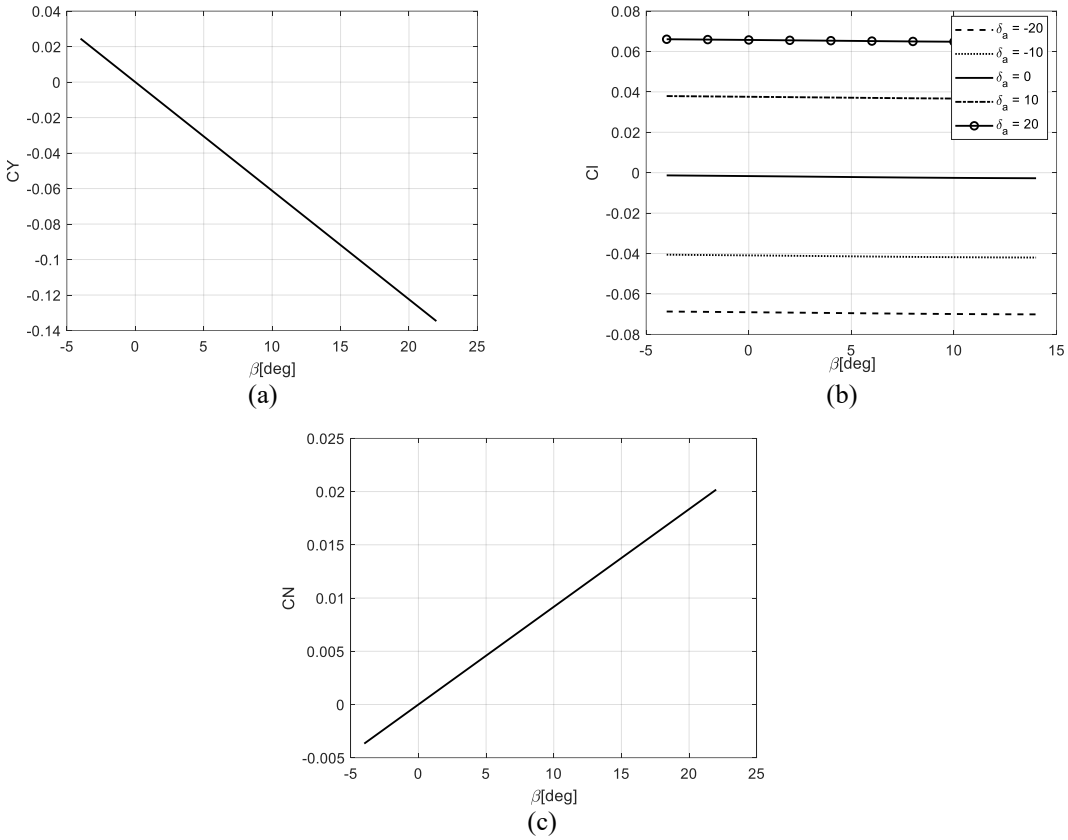

Figure 4. Aerodynamic characteristics of the bMFE-UAV, including the (a) side-force moment coefficient; (b) roll moment coefficient; and (c) yaw moment coefficient.

b. Propulsion

The bMFE-UAV motors are the 3520-500 KV model, with a no-load current of 1.1 A and a resistance of 30 mW. The propellers are two-bladed APC1510 series with 15-inch diameter and 10-inch pitch. The propulsion lines of bMFE, from its two electric propeller engines, have zero incidence angle from the body axis. Therefore, the propulsion only generates forces in the x-body axis, as shown in Eq. (12). The moment equation in Eq. (13), where d_T represents the distance between the thrust and the aircraft's c.g.

$$\bar{F}^P = \frac{1}{2}\rho V_s^2 S_{ref} \begin{bmatrix} C_T\{\delta_T\} + C_{T_u}\hat{u} \\ 0 \\ 0 \end{bmatrix} \tag{12}$$

https://doi.org/10.31436/iiumej.v27i2.4013

$$\bar{M}^P = \frac{1}{2}\rho V_s^2 S_{ref} d_T \begin{bmatrix} 0 \\ C_T\{\delta_T\} + C_{T_u}\hat{u} \\ 0 \end{bmatrix} \quad (13)$$

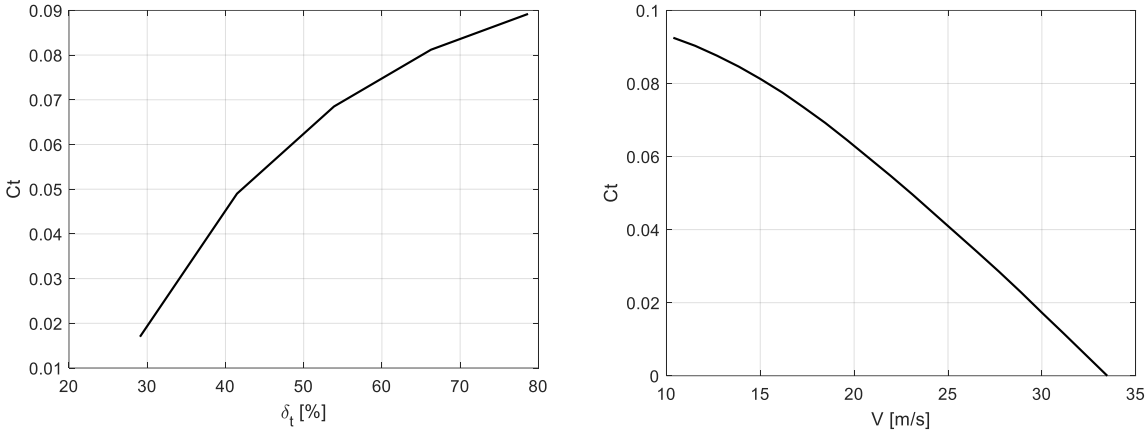

(a) (b)

Figure 5. (a) Thrust Coefficient due to Throttle Deflection; (b) Thrust Coefficient due to velocity.

The propulsion is derived further as a steady-state thrust coefficient C_T, which depends on the throttle input, δ_T, and the dynamic coefficient due to the forward speed u. These are obtained mainly from the bMFE-UAV datasheets and are then shown in **Figure 5**.

c. Gravitational Weights

The last aspect in the definition of the forces in Eq. (7) is the weight aspect, which is modeled as the constant mass (m) multiplied by the gravitational acceleration (g) and transformed to the body axis, as presented in Eq. (14).

$$\bar{F}^W = mg \begin{bmatrix} -\sin\theta \\ \sin\varphi\cos\theta \\ \cos\varphi\cos\theta \end{bmatrix} \quad (14)$$

2.2.2. Non-Linear Simulink Representation

One way to evaluate the vehicle dynamics from the data is to simulate the bMFE-UAV computationally. The equations from Eq. (1) to (14) can be represented using the Simulink Block Set, as illustrated in **Figure 6**. The calculations of the aerodynamic steady-state coefficient are done using the 2-dimensional look-up table block, based on the corresponding aerodynamic angles and control surface deflection.

The UAV dynamic response can be evaluated using this Simulink model, as shown in **Figure 7** for (a) longitudinal and (b) lateral/directional motions. To assess longitudinal dynamics, the UAV model was given a 22° elevator deflection at a steady-state velocity of 15 m/s for 1 s. On the other hand, to trigger the lateral/directional responses, the model was subjected to an 11° aileron deflection doublet for 2 seconds from an 18 m/s steady-state velocity. The values of the initial parameter and the inputs are chosen to match those used in the experiments. Both modes are simulated for 20 seconds, with inputs provided at the 5-second time mark after steady-state conditions are achieved.

Evidently, the responses match the typical dynamic response for conventional aircraft, which are stable in longitudinal and lateral/directional motions. On the longitudinal, two distinguishable stable oscillations can be observed in **Figure 7** (a), which typically are known as the short-period mode oscillation (high frequency – high damping ratio) and the phugoid

mode oscillation (low frequency - low damping ratio). On the other hand, the lateral/directional motions show only one type of oscillation, most likely the Dutch roll mode, which combines stable rolling and yawing motions. This oscillation is most likely accompanied by other stable, non-oscillating motions that are harder to observe in lateral/directional responses in **Figure 7**(b).

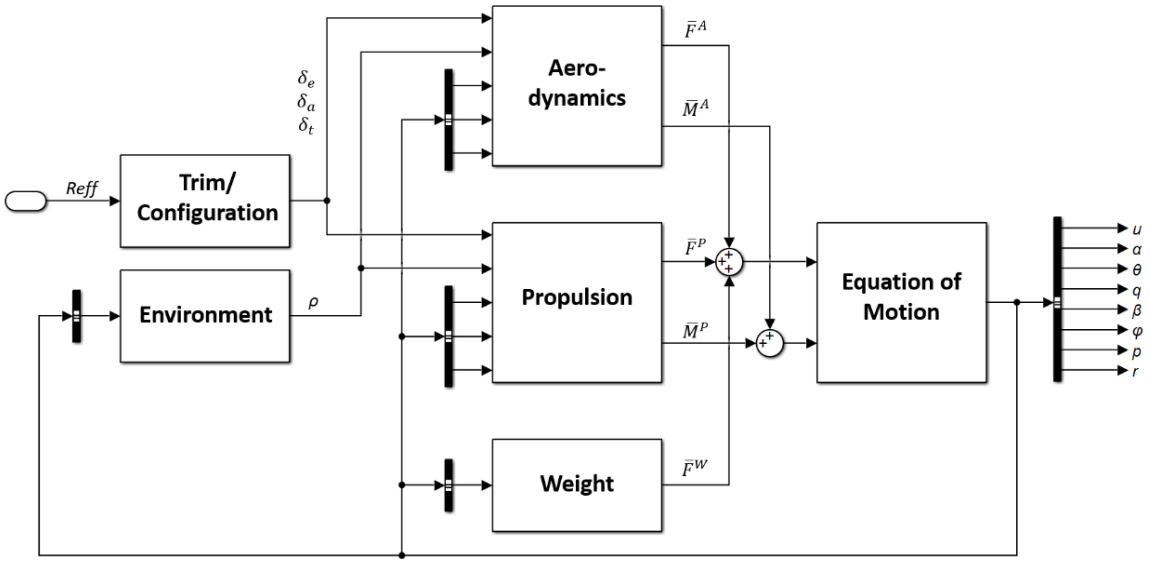

Figure 6. Simulink pseudo-model for the bMFE-UAV dynamics.

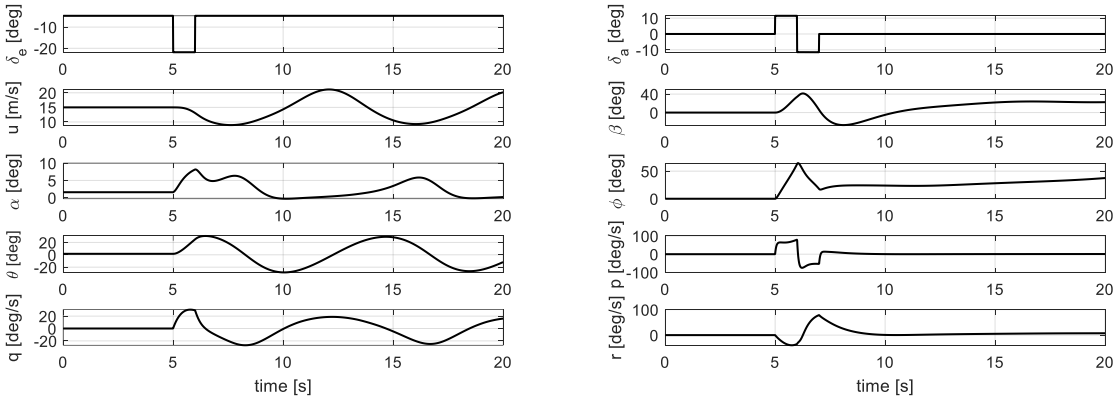

(a) (b)

Figure 7. (a) Longitudinal dynamic responses of the bMFE-UAV; (b) Lateral/directional dynamic responses of the bMFE-UAV

2.2.3. Linear State-Space Representation

Another way to evaluate the bMFE-UAV dynamic response analytically is to retrieve its dynamic parameters from the linearized equation of motion. This can be done using Simulink's Model Linearizer tools, from the previous model depicted in **Figure 6**. Adjusted for the typical states used in aircraft dynamic analysis [17], the linear state-space representation is shown in Eq. (15)-(17) for the longitudinal response, and Eq. (18)-(20) for the lateral directional response.

$$\dot{\bar{x}}_{\text{lo}} = A_{\text{lo}}\bar{x}_{\text{lo}} + B_{\text{lo}}\bar{u}_{\text{lo}},\ \bar{x}_{\text{lo}} = [u \quad w \quad \theta \quad q]^T,\ \bar{u}_{\text{lo}} = [\delta_e \quad \delta_t]^T \tag{15}$$

https://doi.org/10.31436/iiumej.v27i2.4013

$$A_{\text{lo}} = \begin{bmatrix} -0.238 & 0.5468 & -9.802 & -0.3993 \\ -1.167 & -5.283 & -0.2724 & 14.37 \\ 0 & 0 & 0 & 1 \\ 0.1114 & -0.1729 & 0 & -1.954 \end{bmatrix} \tag{16}$$

$$B_{\text{lo}} = \begin{bmatrix} -0.1387 & 0.0934 \\ -1.587 & 0.0045 \\ 0 & 0 \\ -4.607 & -0.0143 \end{bmatrix} \tag{17}$$

$$\dot{\bar{x}}_{\text{ld}} = A_{\text{ld}}\bar{x}_{\text{ld}} + B_{\text{ld}}\bar{u}_{\text{ld}}, \bar{x}_{\text{ld}} = [v \quad \varphi \quad p \quad r]^T, \bar{u}_{\text{ld}} = [\delta_a \quad \delta_r]^T \tag{18}$$

$$A_{\text{ld}} = \begin{bmatrix} -0.296 & 9.8 & -0.223 & -17.999 \\ 0 & 0 & 1 & -0.011 \\ -3.61 & 0 & -15.638 & 5.960 \\ 8.636 & 0 & 5.350 & -10.676 \end{bmatrix} \tag{19}$$

$$B_{\text{ld}} = \begin{bmatrix} 0 & 3.22 \\ 0 & 0 \\ 105.6 & 33 \\ -112.8 & -71.19 \end{bmatrix} \tag{20}$$

Table 3. Dynamic characteristics of bMFE-UAV, obtained from the linearized longitudinal equation of motions

	Parameter	Value
Characteristic Polynomial	$\Delta_{lo} = s^4 + 7.48s^3 + 15.21s^2 + 4.78s + 7.75$	
Short Period	Characteristics Roots	-3.7111 ± 0.710i
	Natural Frequency [rad/s]	3.7785
	Damping Ratio	0.9822
Phugoid	Characteristics Roots	-0.0262 ± 0.736i
	Natural Frequency [rad/s]	0.7368
	Damping Ratio	0.0356

Table 4. Dynamic Characteristics of bMFE-UAV, obtained from the linearized lateral/directional equation of motions

	Parameter	Value
Characteristic Polynomial	$\Delta_{ld} = s^4 + 26.6s^3 + 297.5s^2 + 2162.3s - 114.2$	
Dutch Roll	Characteristics Roots	-5.053 ± 10.230i
	Natural Frequency [rad/s]	11.47
	Damping Ratio	0.445
Roll Subsidence	Characteristics Roots	-16.557
	Half-life time (s)	0.0419
Spiral	Characteristics Roots	0.053
	Doubling time (s)	13.1825

From the dynamic matrices A_{lo} and A_{ld}, the characteristic polynomials of the longitudinal and lateral/directional motion can be derived, from which the dynamics parameter can be obtained. These results are then listed in Table 3 for longitudinal motions and Table 4 for the lateral/directional.

Confirming the results from the non-linear simulation in **Figure 7**, the dynamic parameters from the linearized equation of motion also show typical dynamic responses for a conventional aircraft. Two complex-conjugate pairs of characteristic roots are retrieved in the longitudinal

https://doi.org/10.31436/iiumej.v27i2.4013

direction, as shown in Table 3. These indicate two oscillatory dynamics that match the typical short-period and phugoid modes. While both are dynamically stable, the damping ratio of the phugoid mode might be inadequate under MIL-F-8785C [18], which requires a value greater than 0.04. Therefore, the UAV's flight control system design must place greater emphasis on this mode.

In the lateral/directional direction, a complex-conjugate pair and two real characteristic roots are obtained, as listed in **Table 4**. Similarly, this result aligns with typical lateral/directional dynamics: one oscillatory mode, the Dutch roll, and two non-oscillatory modes, the roll subsidence and the spiral. In this case, the flight control system design needs to account for the spiral mode, which is unstable with a doubling time shorter than the recommended doubling time in MIL-F-8785C. By that standard, the spiral mode can be unstable, but only if the doubling time is more than 20 seconds for the cruising phase.

2.3. Dynamics Characteristics Derivation by Flight Testing

This section elaborates on the dynamic characteristics derived using results from a series of bMFE-UAV Flight Tests. These flight tests were conducted by the Research Center for Aeronautics Technology of the Indonesian National Research and Innovation Agency (BRIN), as shown in Figs. 8, 9, and 10.

Figure 8. Pre-Flight Preparation.

Figure 9. The bMFE-UAV Take-Off Process.

https://doi.org/10.31436/iiumej.v27i2.4013

Figure 10. The bMFE-UAV Flew Successfully.

2.3.1. Flight Test Scenario

The flight tests were conducted under the conditions specified in **Table 5**, with a maximum wind speed of 0.5 m/s. All tests were conducted manually at an altitude of around 300 meters above ground level.

Table 5. Precondition before Taking Off

Parameter at Take-Off	Value
Primary Battery Voltage	25.16 volt
Weight	7.5 kg
CG	0.25 MAC
Starting Time of Flight Test	08.31 WIB
Longitude-Latitude	7°38'59"S 107°41'32"E
Ground Elevation	9 m
Measured Temperature	21 ºC
Wind Speed	0.5 m/s

Table 6. Flight Test Scenario

No.	Mode	Input	Type	Magnitude
1	Longitudinal	Elevator	singlet	+ 15º
2	Lateral/ Directional	Aileron	doublet	+10º, then -10º

Table 7. Flight Test Procedure in Longitudinal Motion

No.	Task	Time (sec)	
1	Trim the aircraft manually and stay in that condition	10	☐
2	Provide elevator singlet input	2	☐
3	Let the aircraft fly freely longitudinally for 10 seconds	10	☐
4	Return to the "race track" pattern so the plane does not leave a controllable visual range	30	☐
	Total execution time	52	

Two test scenarios were conducted, the longitudinal test and the lateral/directional test, as listed in **Table 6**. In the former, a singlet elevator deflection is used to trigger longitudinal dynamics of the bMFE. On the other hand, to induce lateral/directional motion, a doublet aileron deflection is given. The magnitudes, however, cannot always be consistent due to the

nature of pilot control. All flight data is recorded until 12 minutes after the inputs were given. The procedures for the two test scenarios are detailed in Tables 7 and 8.

Table 8. Flight Test Procedure in Lateral/Directional Motion

No.	Task	Time (sec)	
1	Trim the aircraft manually and stay in that condition	10	☐
2	Provide aileron doublet input	3	☐
3	Let the aircraft fly freely for 20 seconds	20	☐
4	Return to the "race track" pattern so the plane does not leave a controllable visual range	30	☐
	Total execution time	63	

2.3.2. Flight Data Result

Figure 11(a) presents the recorded flight data from the longitudinal mode test as deviations from the initial steady-state (trimmed) flight with an airspeed of 15 m/s. Here, the forward speed momentarily decreases after the input is given, then increases, indicating acceleration. Additionally, the angle of attack and pitch angle rise at the beginning but soon stabilize at a consistent value, while the pitch rate tends to return to zero. These results suggest that the aircraft is stable but will drift away from its initial trim condition, even with the elevator input removed.

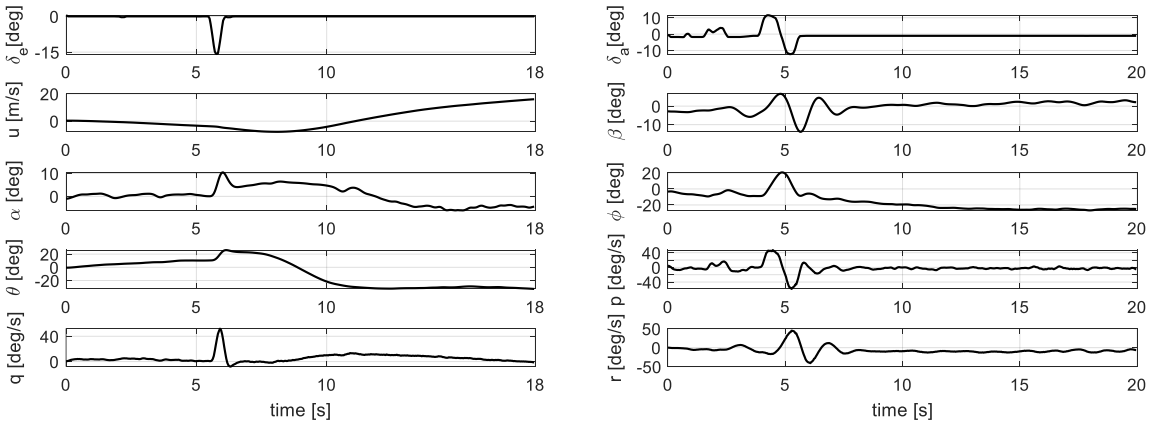

(a) (b)

Figure 11. bMFE-UAV recorded dynamics during flight test, including the (a) longitudinal response due to elevator singlet input (impulse), and (b) lateral/directional response due to aileron doublet input.

Figure 11(b), on the other hand, shows the result of the lateral/directional flight tests of bMFE. In this case, the steady-state velocity recorded is 18 m/s. The doublet aileron inputs were not as clean as preferred, where oscillation is recorded before the intended input. This is likely due to the presence of crosswind from the left, which induced the negative sideslip angle (β) on the steady state condition. In response to the input, the UAV rolled to the right, creating a countering positive sideslip for a short period before returning to the initial trim condition. The roll rate then returned to zero, though not precisely, causing the vehicle to take slightly longer to settle its roll angle.

2.3.3. Parameter Identification

Based on the collected flight test data, a parameter identification process can be performed to obtain the aircraft's dynamic characteristics, such as natural frequency, damping ratio, and half-life. The chosen method for parameter identification is the Ordinary Least Squares (OLS)

[11, 12, 19]. Since the flight data are recorded at discrete time steps, the aircraft state-space equation for motion dynamics, as shown in Eqs. (15) and (18) are reformulated in discrete time as shown in Eq. (21).

$$\bar{z} = H\bar{\theta} + \bar{v} \tag{21}$$

where $\bar{\theta}$ is the vector of the parameters to be identified. The parameter vector estimation is calculated using the OLS error criteria in Eq. (22):

$$\bar{\theta} = [H'H]^{-1}H'\bar{z} \tag{22}$$

The estimated parameters from the OLS method are presented in **Table 9** for the longitudinal mode and **Table 10** for the lateral/directional responses. These parameters include the natural frequency, damping ratio, and half-life time. The confidence intervals and standard errors are also provided to indicate the reliability of the estimates. The composition of complex-conjugate pairs matches the typical modes of aircraft, and thus they are assigned accordingly, as shown in Tables 9 and 10.

Table 9. Dynamic characteristics of bMFE-UAV, obtained from the flight test on the longitudinal responses

Mode	Parameter	Symbol	Value
Short Period	Characteristics Roots	s_{sp}	-1.329 ± 0.582i
	Natural Frequency [rad/s]	ω_{n-sp}	1.4560
	Damping Ratio	ς_{sp}	0.9160
Phugoid	Characteristics Roots	s_{ph}	0.028 ± 0.114i
	Natural Frequency [rad/s]	ω_{n-ph}	0.1168
	Damping Ratio	ς_{ph}	-0.2368

Table 10. Dynamic characteristics of bMFE-UAV, obtained from the flight test on the lateral/directional responses

Mode	Parameter	Symbol	Value
Dutch Roll	Characteristics Roots	s_{dr}	-0.435 ± 4.221i
	Natural Frequency [rad/s]	ω_{n-dr}	4.2435
	Damping Ratio	ς_{dr}	0.1025
Roll Subsident	Characteristics Roots	s_{rs}	-1.6309
	Half-life time [s]	$T_{\frac{1}{2}spi}$	0.4250
Spiral	Characteristics Roots	s_{spi}	-0.5436
	Half-life time [s]	$T_{\frac{1}{2}spi}$	1.2752

Figure 12(a) to (b) shows the comparison between the real data and the estimated data based on the identified parameters. The comparison demonstrates that the estimated model accurately captures the aircraft's dynamic characteristics, with minimal residuals indicating a good fit between the model and the real data.

The coefficient of determination, R^2, is used to assess the proportion of variance in the dependent variable that is explained by the independent variables. A higher R^2 value indicates a better prediction model, signifying that the independent variables jointly explain a large portion of the variation in the dependent variable.

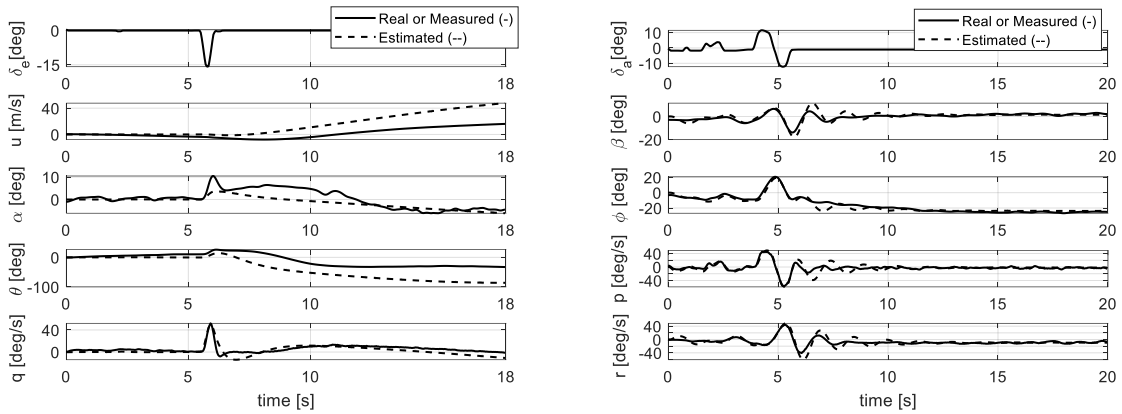

Figure 12. The comparison of real flight test results and the estimated results on (a) the longitudinal mode, and (b) the lateral/directional mode.

Conversely, a lower R^2 value suggests that the independent variables have limited explanatory power [20]. The R^2 value is calculated using the following Eqs. (23) and (24).

$$R^2 = 1 - \frac{\sum_i (y_i - f_i)^2}{\sum_i (y_i - \bar{y})^2} = 1 - \frac{\sum_i e_i{}^2}{\sum_i (y_i - \bar{y})^2} \tag{23}$$

where,

$$\bar{y} = \frac{1}{n} \sum_{i=1}^{n} y_i \tag{24}$$

Table 11. Coefficient of determination and MSE for longitudinal motion variables

Parameter	R^2	MSE
u	0.86	0.013
α	0.72	0.016
θ	0.85	0.017
q	0.66	0.004

Table 12. Coefficient of determination and MSE for lateral/directional motion variables

Parameter	R^2	MSE
β	0.74	0.006
φ	0.93	0.003
p	0.72	0.004
r	0.80	0.003

After calculating the coefficient of determination and MSE, all included variables are considered acceptable, with the pitching rate variables for longitudinal dynamics and the rolling rate for lateral/directional dynamics yielding the lowest values. These indicate that the proposed model, derived from the flight test data, effectively captures a significant portion of the variance in the dependent variables, using the selected independent variables. The lowest MSE indicates that the average prediction error is small.

3. Results Comparison and Analysis

Tables 13 and 14 compare the results of bMFE's dynamic characteristics derived from analytical calculations and flight-test data identification.

3.1. Overall Comparison

Generally, the analytical method is expected to offer a clear, systematic approach grounded in theory and to provide a strong foundation for the final design and stability analysis. However, it may not account for all real-world variables and disturbances. On the other hand, the flight test combined with the OLS identification method leverages actual flight data, capturing real-world dynamics but potentially introducing noise and experimental errors.

Table 13. The difference in longitudinal dynamic characteristics between the analytical and the flight test method

Parameters		Results		Difference (from analytical)
		Analytical	Flight Data	
Short Period	s_{sp}	-3.711 ± 0.710i	-1.329 ± 0.582i	-
	ω_{n-sp}	3.7785 /s	1.4560 /s	61.4%
	ς_{sp}	0.9822	0.9160	6.1%
Phugoid	s_{ph}	-0.026 ± 0.736i	0.028 ± 0.114i	-
	ω_{n-ph}	0.7368 /s	0.1168 /s	84.1%
	ς_{ph}	0.0356	-0.2368	-

Table 14. The difference in lateral/directional dynamic characteristics between the analytical and the flight test method

Parameters		Results		Difference (from analytical)
		Analytical	Flight Data	
Dutch Roll	s_{dr}	-5.053 ± 10.30i	-0.435 ± 4.221i	-
	ω_{n-dr}	11.47 /s	4.244 /s	63.0%
	ς_{dr}	0.445	0.103	76.4%
Roll Subsidence	s_{rs}	-16.557	-1.6309	-
	$T_{\frac{1}{2}_{rs}}$	0.0419 s	0.4250 s	914.3%
Spiral	s_{spi}	0.053	-0.544	-
	$T_{\frac{1}{2}_{spi}}$	(13.1825 s)*	1.2752 s	-

* Doubling-time

As listed in Tables 13 and 14, both methods consistently yielded oscillatory behavior, enabling the assignment of typical aircraft modes. In the longitudinal mode, two oscillatory modes are observed, as indicated by the two complex-conjugate pairs. In the lateral/directional case, both methods yielded complex-conjugate pairs together with two real roots. This manifested in the lateral/directional time response as a single oscillatory motion, accompanied by two non-oscillatory components (see **Figure 12**).

Evidently, only the damping-ratio results for the Short-period mode show close agreement, with a difference of less than 10%. Others, including the Short Period's natural frequency, displayed significant discrepancies between the methods' results. However, the flight test method consistently gives a lower oscillation frequency and a longer half-life. The lack of an actuator dynamic model in the analytical method calculation might cause these. Actuator dynamics should introduce delays and phase lag, which can reduce the natural frequency, as shown by a shift in the real parts of the characteristic roots to the left of the complex plane. The damping ratio, especially for the Short-period mode, might not change as much because it is more affected by aerodynamic factors. Other reasons for these discrepancies can include

https://doi.org/10.31436/iiumej.v27i2.4013

inaccuracies in mass and inertia distribution, the lack of a structural flexibility model, or nonlinear effects.

Moreover, the discrepancies shown are not limited to the value of dynamic parameters but also to stability. For instance, the results in the Phugoid mode indicate that the analytical method predicts the UAV is stable, whereas the flight test indicates instability. **Figure 12**(a) shows that instability happens when the vehicle's forward speed, which is a dominant factor for phugoid mode, increases by more than 40 m/s from the initial 15 m/s airspeed. In this condition, the assumption of linearity of the aerodynamic derivative cannot hold, leading to stability inversions.

On the other hand, the spiral mode produced a different result: the analytical method yielded an unstable result, whereas the flight data showed stability. This result indicates that some unknown damping factors may not yet have been accounted for in the analytical model. Another reason is that since the damping in the rolling and yawing rates is higher in the flight test result, the roll angle range is much more limited, only from -20º to 20º. In contrast, the roll result is nearly 60 ° to the right in the analytical method. This difference in roll envelope may contribute to the discrepancies observed in the lateral/directional stability results.

3.2. Steps in Derivation Process

To derive the dynamic characteristics of the bMFE UAV, the analytical approach requires significantly more steps than the flight test method. In modeling, each factor and its derivatives with respect to the six motion parameters need to be derived. Aerodynamics alone requires at least twelve static and dynamic derivatives, not to mention the control derivatives. Using software like the USAF DATCOM can reduce the time required, but only if all aircraft configurations and flight conditions are well-defined. The process of finding the Center of Gravity and Inertia can also pose a challenge for an off-the-shelf UAV, as it often requires numerous experiments.

Additionally, deriving the propulsion effects for an already installed system is complex. The more accurate the model needs to be, the more effort is required to determine each factor. However, from the facility's point of view, all this can be done in a laboratory using a single good computer. On the other hand, flight testing coupled with an identification process is more straightforward. Flight testing for an off-the-shelf small UAV can be conducted immediately, yielding enough data to support an identification process. Moreover, the results can represent the entire configuration and conditions during the flight test in a single all-in-one experiment. The most essential requirement is an experienced pilot who can establish an initial trim condition, apply the input correctly, and let the plane fly freely to be recorded, while avoiding collisions and crashes. However, this method also requires a flight test field and fair and consistent weather conditions.

Nevertheless, for a small UAV, this research has shown that it is more practical and efficient to focus on the flight-test and identification approach for deriving dynamic characteristics. Small UAVs such as the bMFE-UAV can be quickly deployed and flown, making it easier to gather flight-test data without extensive preparatory work. The flexibility to repeat flight tests under different conditions also facilitates the design of robust control systems capable of handling various scenarios.

3.3. Implications in Designing the Automatic Flight Control System for Small UAVs

The comparative analysis between the analytical and flight test methods highlights the practical advantages of the latter approach. For small UAVs already built and available for

immediate use, the flight test method offers a straightforward way to identify the vehicle's dynamic characteristics. As the UAV is flown repeatedly and the flight test data is consistently obtained, the accuracy of the derived characteristics improves over time. This tendency implies that control system design, such as pitch hold, altitude hold, and stability augmentation, can be further refined through additional flight tests.

Some concerns exist regarding differences in dynamic parameters obtained from the flight-test method compared with the analytical approach. These discrepancies may warrant further investigation. However, despite these differences, the flight test method remains more practical for designing flight control systems. Ensuring that analytical and flight test results align precisely may not be as crucial as the immediate benefits of the flight test method for practical control system design.

The flight test method is a part of the data-driven approach, which is not only becoming increasingly common but also more viable and promising due to advancements in sensor technology and data processing capabilities. This approach leverages real-time data to provide accurate and up-to-date insights into the UAV's performance. As sensors become more sophisticated and accessible, the ability to gather detailed flight data has improved, making the data-driven approach more viable and effective for UAV control system design. This method is particularly suitable for small fixed-wing UAVs, which have also become more accessible and cheaper, further enhancing the practicality and appeal of the data-driven approach.

4. CONCLUSIONS

UAV dynamic parameters for a small fixed-wing UAV, the bMFE-UAV, have been derived using two approaches. The first approach is analytical, utilizing a mathematical model derived from physical principles with data from the USAF DATCOM. The second approach involves flight testing and data analysis using Ordinary Least Squares (OLS). The results include parameters such as damping ratio and natural frequency, from which flight modes can be identified. These results have been compared, and both methods have yielded consistent oscillatory behavior, enabling the assignment of typical aircraft modes. Only the short-period mode shows close agreement, with a difference of less than 10%. Others, including the short-period's natural frequency, displayed significant discrepancies between the method's results. The observed discrepancies underscore the inherent limitations of analytical methods in capturing the complexity of real flight dynamics. Accordingly, this research provides empirical evidence that flight testing remains indispensable, as it produces reliable data to support the design, validation, and fine-tuning of small UAV flight control systems.

ACKNOWLEDGMENT

The research was supported by Research Center for Aeronautics Technology, National Research and Innovation Agency, Indonesia and was conducted as part of the Development of Flight Control and Guidance Systems for Advanced Vehicles research, under the 2021 - Penelitian, Pengabdian Masyarakat dan Inovasi (P2MI-2021) program of Flight Physics Research Group, Faculty of Mechanical and Aerospace Engineering, Institut Teknologi Bandung.

REFERENCES

[1] Dimitriadis G., Panagiotou P., Dimopoulos T., & Yakinthos K. (2024). Aerodynamic Stability Derivative Calculations Using the Compressible Source and Doublet Panel Method. Journal of Aircraft, 61(4), 1034-1046. https://doi.org/10.2514/1.C037747.

[2] Okhovatian S., & Koukounian V. (2024). Using Empirical Data to Validate the Role of Computational Fluid Dynamics in Various Stages of Aero-Acoustic Simulations. Canadian Acoustics - Acoustique Canadienne, 52(1). https://doi.org/10.1121/10.0026809.

[3] Liu Y. (2023). Harnessing CFD Modeling Techniques for Optimizing Automotive Streamlines and Reducing Aerodynamic Drag. Highlights in Science, Engineering and Technology. https://doi.org/10.54097/v25ka918.

[4] Olejnik A., Dziubiński A., & Kiszkowiak Ł. (2021). Reliable method of aerodynamic analysis using computational fluid dynamics and scaled models in the development process of a Very Light Airplane. IOP Conference Series: Materials Science and Engineering (1), 1024. https://doi.org/10.1088/1757-899X/1024/1/012048.

[5] Tai S., Bu C., Wang Y., Yue T., Liu H., & Wang L. (2024). Identification of aircraft longitudinal aerodynamic parameters using an online corrective test for wind tunnel virtual flight. Chinese Journal of Aeronautics, 37(9), 261-275. https://doi.org/10.1016/j.cja.2024.05.031.

[6] Corneliu S., Burghiu M., Trandafir E., Apostol E., Nica A., Pana A., Balasa R., Curt D., Defta S., Vajaiac E., Pirvu C. (2023). Wind Tunnel Testing of a Common Research Model. INCAS Research Challenges in Aerospace Technologies. https://doi.org/10.2514/6.2023-1017

[7] Benyamen H., Benjamin S. Mays. Chowdhury M., Keshmiri S., & Mark S. (2023). Analysis of Aircraft Simulation Validity in Different Flight Conditions. International Conference on Unmanned Aircraft Systems. https://doi.org/10.1109/ICUAS57906.2023.10156586.

[8] Xu S., Bi W., Zhang A., & Mao Z. (2022). Optimization of flight test tasks allocation and sequencing using genetic algorithm. Applied Soft Computing, 115. https://doi.org/10.1016/j.asoc.2021.108241.

[9] Weishaeupl A. B., Scanlan J., & Sobester A. (2023). Flight Test Driven Development of Low Cost UAVs - Pitfalls and Opportunities. AIAA 2023-1739. https://doi.org/10.2514/6.2023-1739.

[10] Mohd Shah H. N., Mohamad Sebir M. A., Abdollah M. F., Baharon M. R., Ahmad A., & Ali Arshad M. (2023). Develop and Design Small Scale UAV. Modern Applied Science, 17(2), 49. https://doi.org/10.5539/mas.v17n2p49.

[11] Jategaonkar R. V. (2006). Flight Vehicle System Identification (978-1-62410-279-0 ed.).

[12] Klein V., & Morelli E. A. (2006). Aircraft System Identification: Theory and Practice.

[13] Wang L., Zhao R., & Zhang Y. (2022). Aircraft Lateral-Directional Aerodynamic Parameter Identification and Solution Method Using Segmented Adaptation of Identification Model and Flight Test Data. Aerospace, 9(8). https://doi.org/10.3390/aerospace9080433.

[14] Ali S., Hassan O., Gopalakrishnan A., Muriyan A., & Francis S. (2022). Unmanned Aerial Vehicles: A Literature Review. Hunan Daxue Xuebao/Journal of Hunan University Natural Sciences, 49(7), 96-113. https://doi.org/10.55463/issn.1674-2974.49.7.11.

[15] Dias J. N. (2023). Flight-Test Determination of Longitudinal Stability Using System Identification. Journal of Aircraft, 60(5), 1659-1674. https://doi.org/10.2514/1.C037252.

[16] Fighter Hand launch fixed wing [https://diydrones.com/profiles/blogs/fighter-hand-throw-fixed-wing].

[17] Roskam J. (2001). Airplane Flight Dynamics and Automatic Flight Controls - Part 1.

[18] Departments and Agencies of the Department of Defense. (1980). Military Specification Flying Qualities of Piloted Airlines.

[19] Li H. (2024). Aerodynamic parameter identification method of unmanned aerial vehicles (UAVs), (p. 115). https://doi.org/10.1117/12.3039610.

[20] Chicco D., Warrens M. J., & Jurman G. (2021). The coefficient of determination R-squared is more informative than SMAPE, MAE, MAPE, MSE and RMSE in regression analysis evaluation. PeerJ Computer Science, 7, 1-24. https://doi.org/10.7717/PEERJ-CS.623